

# Optimization of Friction Stir Processing Parameters for AA 6061-Polypropylene Reinforced Composites using the Taguchi Analysis

Mohd. Muzammil Uddin<sup>1</sup>, M. Thirumurugan<sup>2</sup>

<sup>1,2</sup>*Welding and Manufacturing, Crescent Institute of science and Technology, Hyderabad, India*

**Abstract** - The traverse speed, tool tilt angle, and rotational speed of friction stir processing all have an effect on the strength of the processed area. As a result, these process parameters may be chosen and configured correctly to maximise the processed zone's strength. Taguchi's work aims to optimise process parameters such as traverse speed, tool tilt angle, and rotational speed in order to increase ultimate tensile strength in aluminium 6061 sheets with a thickness of 10 mm and a polypropylene granule content of 5%. Additionally, the three components on three levels are employed as the Taguchi technique's orthogonal L9 array. ANOVA was used, as well as validation tests. The results demonstrate that the rotational speed, traverse speed, and tool angle all have an effect on the FSP strength. The highest strength intensity was 16.06 MPa, and optimization data revealed 40 mm/min, 1420 rpm, and a 1° tool angle, traverse speed, and rotational speed.

**Index Terms** - Friction stir processing; Microstructure analysis; Taguchi analysis; Polypropylene; ultimate tensile strength.

## 1. INTRODUCTION

The energy crisis, for example, in energy consumption and environmental pollution, is becoming increasingly imminent recently, particularly in automotive, electronics and other industrial sectors. The lightweight material used in an automobile is now one of the most significant ways of saving energy and reducing emissions, including magnesium alloy [1], Aluminium alloy and polymers. The aluminium alloy-based polymer hybrids [2,3] will satisfy the needs of a wide range of properties of the products, but also reduce the weight of the product considerably. This is valuable for applications in which the original features of the material must be retained. Key friction stir processing (FSP) parameters for flow of material, heat

intake, processing speed, speed of tool, tilt angle, axial force and geometry of tools affect the processed region's consistency [5-7]. Although the FSP method was initially developed to process Al-alloys [8-11], it also offers a lot of promise for processing magnesium, titanium, steel, metal matrix composites, and other material combinations [12-17]. Numerous researchers have subsequently investigated FSW and friction stir spot welding (FSSW) for polymers and polymer composites [18–20]. According to prior research, FSP has mostly been utilized to treat metals and metal alloys. As a result, it is worthwhile to study the capability of this technique for processing aluminium (AA6061) composites reinforced with 5% polypropylenes (PP). Although research has been undertaken on friction stir butt welding of polypropylene composites [20], no reports on friction stir processing of aluminium 6061 with polypropylene composite by FSP have been published. The purpose of this study is to look at the impact of FSP parameters on the ultimate tensile strength of aluminium 6061 with 5%wt polypropylene granules. As a general polymer, polypropylene (PP) is also used in automobiles, electronics, and in other industries. The lightweight and strong mechanical characteristics of aluminium alloy are commonly used. However, the direct bond tensile strength of polypropylene and aluminium alloys is only 1.6 MPa, which clearly does not meet product efficiency criteria [21]. Nevertheless, previous research has been carried out with compression-molded processing technology to investigate bonding properties in aluminium alloy / modified polypropylene (PPs) hybrids and maximum tensile strength in a sample of PMH has been reached at 10 MPa [22-23]. To increase the tensile strength of hybrid polypropylene-aluminium alloy specimens via

an orthogonal test configuration and modes of failure in the hybrid polypropylene/aluminium alloy samples, the rotational speed, cross speed, and angle of the tool processing parameters were carefully examined.

## 2.METHODOLOGY AND EXPERIMENTAL PROCEDURE

RS, TS and TTA [7] are the parameters of FSP process which can affect quality and performance of FSP joints. Three levels of these process parameters were investigated in this investigation after trial runs were conducted. The experimental parameter ranges have been determined in a manner which produces an appropriate processed region. Figure 3 display unacceptable zones generated outside working ranges of parameters at a certain process stage. Table 1 provides the parameters of the FSP process and their rates.

Table 1. Parameters I and levels for the FSP phase

Symbol	Processing parameter	Unit	Level 1	Level 2	Level 3
RS	Rotational speed	rpm	710	1120	1400
TS	Traverse speed	mm/min	30	35	40
TTA	Tool Tilt angle	degree	0	1	2

## 3. MATERIALS AND EQUIPMENT

Indian oil and corporation limited (India), whose physical parameters were seen in Table 2, were equipped with isotactic polypropylene. Aluminium sheets (A6061), which are the major chemical compounds of Al98.48 %, Mg 0.90 %, and Si 0.62 %, were supplied by Andhra steel suppliers (Hyderabad, India), and aluminium alloy sheet was cut down into 130 mm x I 80 mm x 10 mm each for any experimental sample.

Table 2. Polypropylene's physical properties.

Density (g/cm3)	Melt Index (g/10 min)	Vicat Softening Point in (°C)	Shrinking Percent (%)	Tensile Strength (MPa)
0.92	13.5	119	1.5-21	32

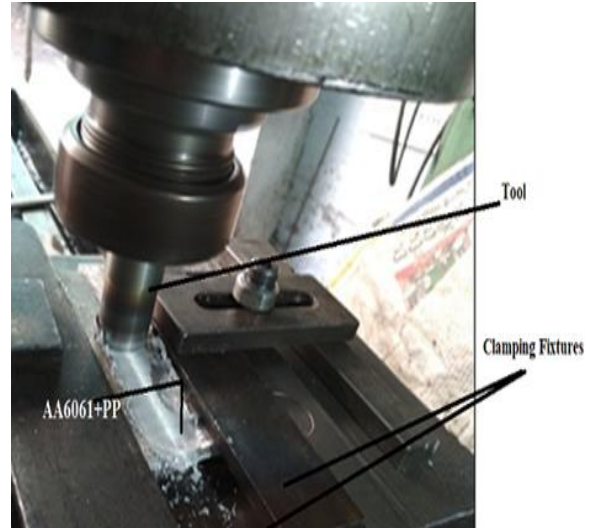


Fig.1. Arrangement of the spanner, aluminium plate and tool used.

Before being filled in blind troughs of a plate with aluminium, the PP granules were dripped on a vertical milling machine for 20 minutes using a clamping attachment as seen in Figure 1.

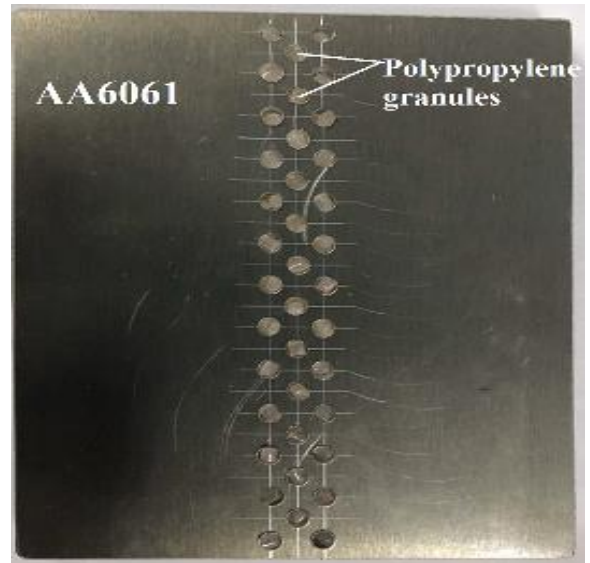


Fig. 2. Aluminium 6061 and polypropylene granules filled in blind holes

The test was conducted with a I cylindrical-conical I raised pin tool found in Fig. 4. The tool instrument is made of tool steel (H13) and heat is heated to 58 HRC with a shoulder 18 mm diameter, pin 5 mm diameter and 5.5 mm in height.



Fig. 3. Conical threaded tool pin profile used for experimental work

Taguchi concept mathematical technique was chosen to analyse the impact of the UTS joints phase parameters. The experimental design steps of the Taguchi include: (a) optimization of the response (output variable), (b) the identification of the factors (input variables). the following: (c) choice of the I appropriate orthogonal I array; (d) assignment of factor to columns in the array; (e) random experimentation to minimize systemic errors; (f) the results are verified using the SN ratio and variance analysis (ANOVA); (g) the method process parameters are determined and confirmations are performed [34].

### 3.1 Specimen preparation for tensile strength testing

After processing in line with the ASTM E8/E8M-11 standard [35], the specimens with measurements shown in Fig. 5 have been prepared from the center of the refraction mixers to prevent the processing beginning and ending results. UTS experiments with a universal testing machine for nano plug-in hydraulics have been performed with the crosshead speed at 1mm/min when loading.

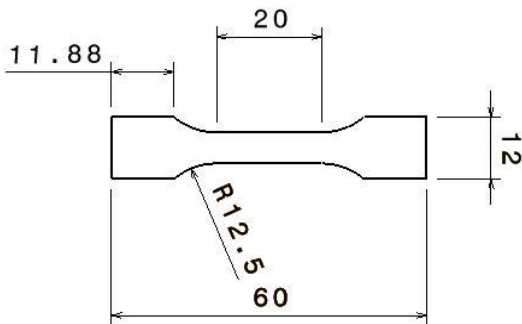


Fig. 4. Tensile test specimen geometry and dimensions (mm).

### 3.2 Microstructure structure examinations

Sample surface microstructure and topography, including surface and aluminium alloy surface of fractured specimens was investigated with a field scanning electron microscopy (FESEM, Osmania University campus, Hyderabad, INDIA). In addition, a scanning electron microscope characterized the morphology of the tensile fracture. In order to identify the filling PP / FESEM aluminium alloy interface, cross segments of the samples were studied.

## 4.RESULTS & DISCUSSION

### signal-to-noise ratio

The response or attribute considered in this work to characterize the consistency of the FSP joints is ultimate tensile strength. The mean and SN ratios for each process parameter must be determined to ascertain the effect of process parameters on this response. The SN ratio is the desirable signal ratio according to the Taguchi process, i.e., a medium of output characters and noise that is the un-acceptable value, i.e., square variance of output characteristics. The SN ratio is also known as the average to square deviation ratio. Taguchi employs the SN ratio [36] to account for output characteristics that differ from the optimal value. It is described by  $\eta$ ; its unit is I dB, and its defined as [24]:

$$\eta = -10 \log (M.S.D) \quad (1)$$

where M.S.D. denotes the output, characteristic's mean I square variance.

Taguchi distinguishes I three types of consistency in I the SN ratio: less the better, much greater the I better and nominal the better. The S / N ratio is calculated using SN analysis for each method parameter. Regardless of the type of I quality I characteristics a higher SN ratio with better I quality I characteristics is associated. The optimum process parameter was previously known to be the maximum quantity of the SN ratio [38]. The SN I ratio was selected to maximise the manufactured UTS based on the greater-the-better requirement (response). For better consistency, the M.S.D is expressed as [24].:

$$M.S.D = \frac{1}{n} \sum_{i=1}^n \frac{1}{T_i^2} I \quad (2)$$

where n denotes the I number of I tests and  $T_i$  denotes the processed power of I the  $i^{th}$  measure. In this analysis, 9 UTS values and 9 SN ratio values were

obtained. The mean and SN ratios have been calculated to evaluate the effect of processing parameters on UTS for each processing parameter. As seen in Table 3, a frictional sorting of the plate took place at random. The findings for UTS and the corresponding SN ratios as calculated using Equations (1) and (2). For calculations on the I effect of the FSP method parameters on the average SN ratios in respect of the type of the I experiments shown in Table 4, the MINITAB-15 statistical Programme.

Table 3. Experimental data for UTS.

Exp. no.	Input parameter			UTS (MPa) (Mean)	SN ratio for UTS (dB)
	RS (rpm)	TS (mm/min)	TTA (degrees)		
1	1	1	1	15.14	23.60
2	1	2	2	14.86	23.44
3	1	3	3	15.57	23.85
4	2	1	2	15.78	23.96
5	2	2	3	14.89	23.46
6	2	3	1	15.81	23.98
7	3	1	3	15.61	23.87
8	3	2	1	14.97	23.50
9	3	3	2	16.06	24.11

Fig. 5 shows that the maximum value for RS, TS and TTA were respectively at levels 3, 3 and 2, in the main results for SN ratios, i.e., RS3-TS3-TTA2. Since the experimental architecture is orthogonal, each processing parameter can be divided into three stages. For example, in average SN ratios for RS in Level 1, 2, and 3, the average SN ratios of tests 1-3, 4-6 and 7-9 can be calculated [19] respectively. The average SN ratio for each processing parameter stage as shown in Table 3. All nine experiments showed a mean SN ratio of 23,75 db.

Table 4. The I mean SN I response I table for UTS.

Symbol	Mean SN ratio (dB)				
	Level 1	Level 2	Level 3	Delta	Rank
RS	23.63	23.80	23.83	0.20	2
TS	23.81	23.47	23.98	0.51	1
TA	23.70	23.84	23.72	0.14	3

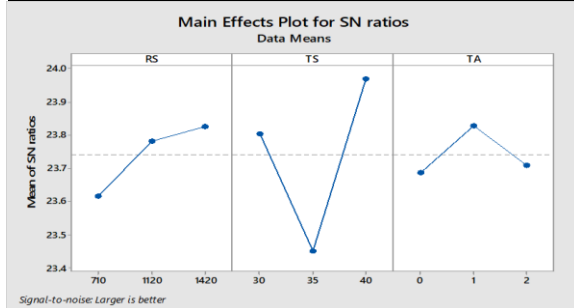


Fig.5. The plot of the main effects for the SN ratio.

Table 5. The ANOVA results for UTS

Symbol	DoF	SS	MS	F	P	Contribution as a Percentage (%)
RS	2	0.22207	0.111033	22.06	0.043	13.67
TS	2	1.27807	0.639033	126.96	0.008	78.68
TTA	2	0.11420	0.057100	11.34	0.081	7.03
Error	2	0.01007	0.005033			6.20
Total	8	1.62440				100

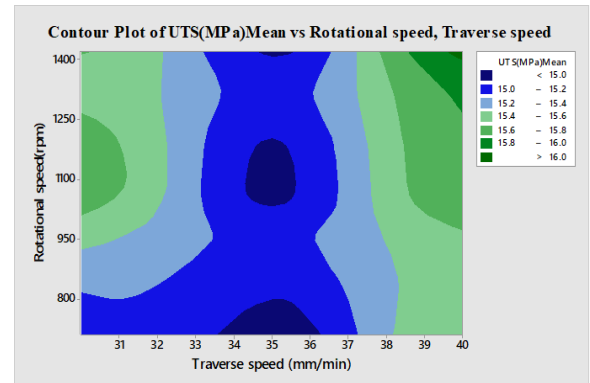


Fig. 6. The influence of TS and RS on UTS is represented by a contour plot

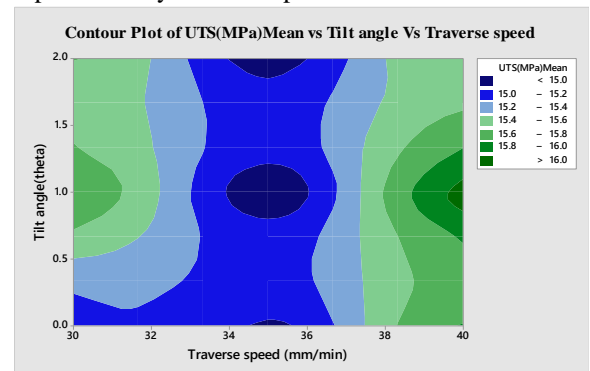


Fig. 7. The contour plot depicts the influence of TS and TA on UTS

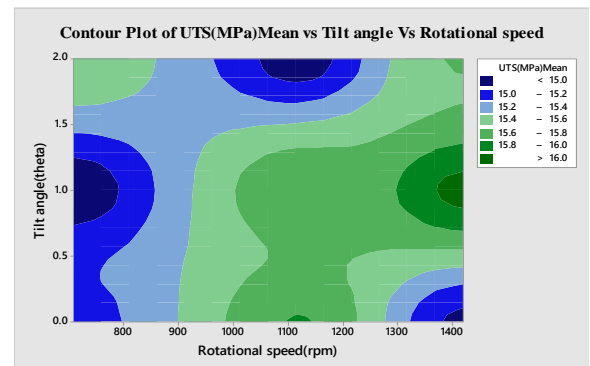


Fig 8. The contour plot represents the influence of RS and TA on UTS

The contour plots of Figs. 6-8 display the effect of the FSP processing parameters on the UTS, according to the findings shown in Table 3. The MINITAB-15 Programme was used to create these contour plots for the Taguchi process.

The full UTS region is represented by all of the dark green regions in the graphs. Full UTS can be achieved at high processing speeds (40 mm/min and higher) and high rotational speeds (1400rpm and higher), as seen in Fig. 7. Figures 7 and 8 display comparable effects. It is clear from figure 6 that ultimate tensile strength increases as the rotational speed and traverse speed increases this is due to the homogeneity of the composition of mixture as clearly seen in figure 12.

4.1 Analysis of variance

Variance analysis may be used to assess the relative impact on processed strength of the processing parameters. When determining the optimal combination step, the relative value of the parameters is crucial [39].

Table 5 shows the ANOVA findings for the mean UTS. The f-test was employed to see if the process parameters were significant. Considerable changes in processing parameters (or methodologies) lead to significant changes in ranking [39]. It is likely that the examined processing parameters have a large impact on the UTS in the FSP joints.

4.2 Percentage contribution

The percentage contribution of a factor shows its relative ability to minimize variance. A slight difference in a factor with a higher percent contribution would have a large impact on results [39]. Table 5 and Figure 9 display the percent contribution of the processing parameters to the UTS. It has been discovered that TS is the most critical processing parameter influencing weld power. In this analysis, TS was a significant element, while TA was a small one. TS is the most significant component of FSP that affects processed power, accounting for 79.06 percent of the total. Just 0.03408 of the variances were caused by experimental flaws, demonstrating that the experimental design was extremely accurate.

Table 6. Confirmation test results for UTS

Optimum conditions in production		
	Prediction	Experiment
Parameter levels	RS3, TS3, TTA2	RS3, TS3, TTA2
UTS (MPa)	16.11	16.08
SN ratio (dB)	24.15	23.91

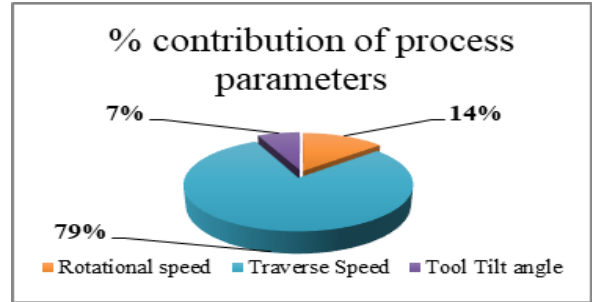


Fig.9. Percent contribution for FSP process parameters

4.3 Validation test

Once the optimal level of processing parameters is chosen, the final stage is to predict and verify the characteristic quality using the optimal level of processing parameters. The expected SN ratio  $\hat{\eta}$  may be calculated as follows:

$$\hat{\eta} = \eta_m + \sum_{i=1}^O (\eta_i - \eta_m) \tag{3}$$

$\eta_m$  is the total mean SN ratio,  $\eta_i$  the mean SN ratio at the optimum level, and O is the number of the main design parameters that affect the quality characteristic. Table 6 provides a comparison, using optimum processing parameters, of the expected and the individual processed UTS. Good consensus is observed between the UTS prediction and actual processed zone.

4.4 Surface characterization

To understand the mechanism of binding of a typical interface of polypropylene and aluminium alloy, SEM with line scan analytics were engaged to analyze the nuclear diffusion and microstructure at the interface. The intersectional and atomic migration micrographs caused by various processing conditions at the friction stir interface are illustration of Fig. 11.

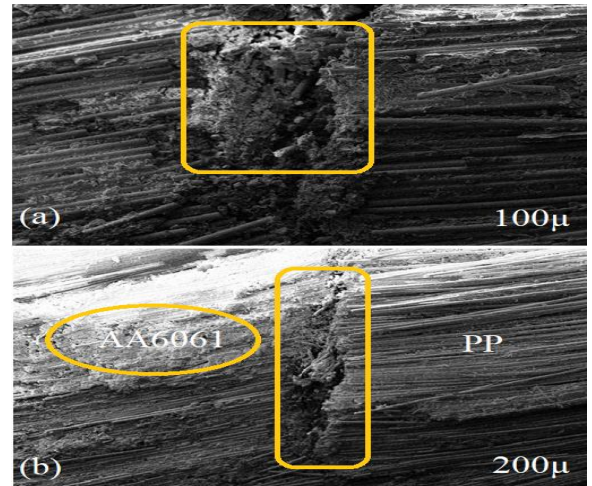


Fig.10(a) and 10(b). shows the interface gap in the cross-section of AA6061 and polypropylene  
 The transverse-coordinate of the sample is the scanning location. The element content can be qualitatively determined by the cps pattern. The interface gap in the cross-section view of the predicted sample is relatively apparent, as Figure 11a shows. It suggests that the interface between the PP and aluminium alloys during the FSP has few micro-interlocking structures. The interface gaps for the sample as seen in Figure 11b, processed under optimized processing conditions and the PP-resin and aluminium alloy, as shown in Figure 11b, are nearly closed at the optimized sample interface.

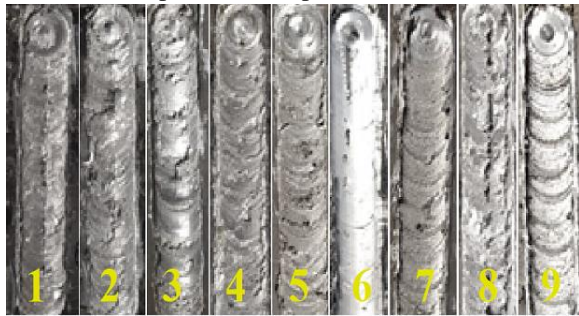


Fig. 11. Aluminium 6061 processed through Taguchi L9 approach

Following a thorough evaluation of the microstructural images of the defect-free joints, it was observed that the size of the grains present in the stir zone is significantly different.

The close interface or optimized sample indicates that the majority of the PP resin has flowed into the Al-surface micro holes and has strong adhesion as compared to the predictions and confirmation samples.

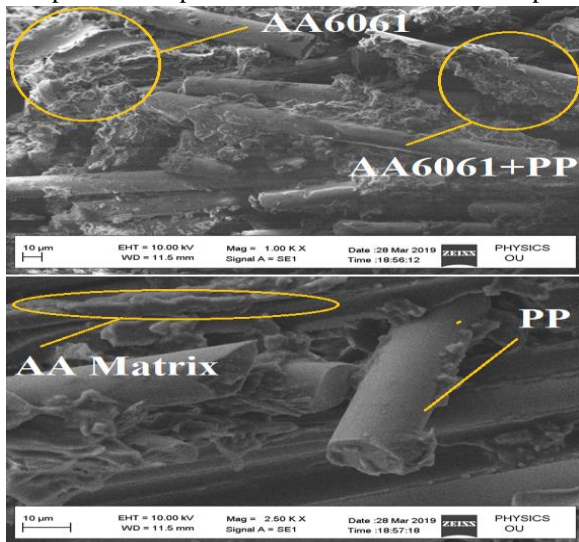


Fig.12. shows the atomic migration of aluminium and polypropylene hybrid.

It is thought that a considerable amount of PP resins migrates through the needle-shaped and forming interlocking microstructures, which are primarily attributed with a high joint strength for the best processed specimen. A line scanning chemical analysis confirms the diffusions of aluminium and carbon atoms at the PP and Al interfaces, which may explain chemical reactions at the FSP sample interface. Since atomic migration in C and Al is rare at interfaces, the precise interface of the reported sample is mainly determined by the VanDerWaals force, which is why the expected sample lacks the poor bonding properties.

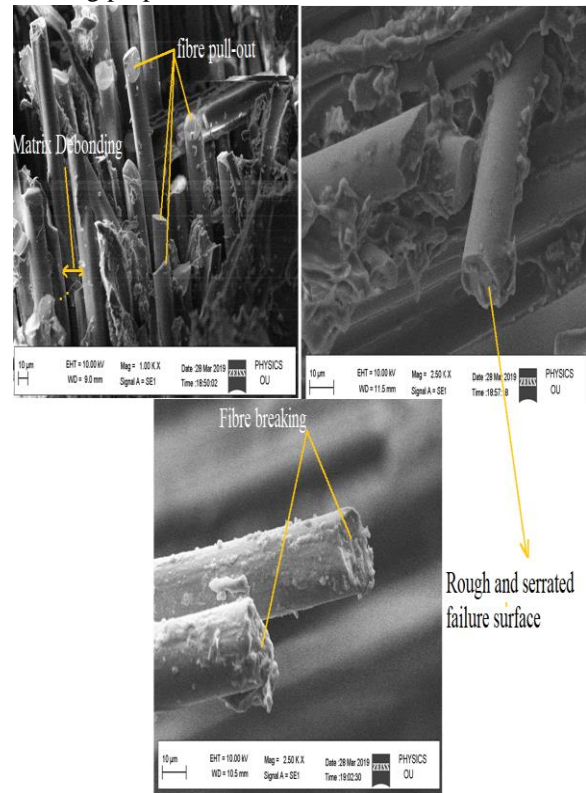


Fig.13.shows the fibre de-bonding/ fibre breaking and fracture surface of polypropylene matrix.

This refers to the report of the former investigator [40,41]. kimiaki et al. [40] used the friction lap welding to reinforce PA6 directly into aluminium Wet grinding procedure alloy and the findings have shown that the working group-NH and -CH in PA6 formed chemical bonds, resulting in optimum strength for the metal surface oxides and Al OH)<sub>3</sub>.

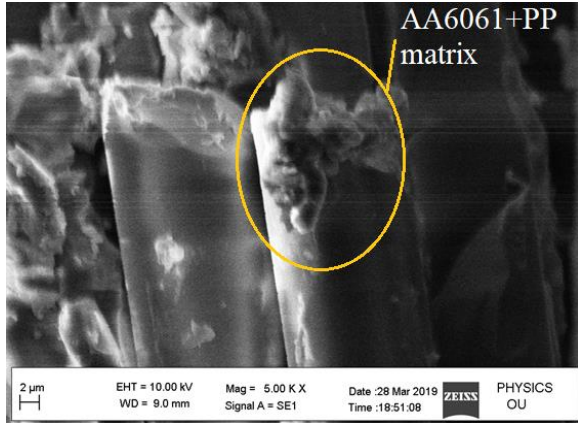


Fig.14. Fibre debonding at 2µm

Chen et al. [41] addressed the effects on aluminium / PP / aluminium foil shear after surface pre-treatment with sandpaper grinding aluminium sheet, on maleic anhydride grafting amounts in polypropylene. It has shown that the Chemical interactions with the NH<sub>2</sub> - OH, Al<sup>3+</sup>, and the interface between the anhydride group of the polar feature and carboxyl groups -COOH on the surface of aluminium sheets have resulted in extreme plastic polymer deformations.

### 5.CONCLUSIONS

The following results can be taken from this work

1. The ultimate tensile strength of Polypropylene / 6061 Aluminium alloy hybrids were developed in the work using the Friction stir processing (FSP), while the maximum predicted ultimate tensile strength for the hybrid processed after confirmation test was up to 16.08 MPa at the optimal processing parameters.
2. Furthermore, the optimum processing parameters were established by the orthogonal experimental design for developing the strong polypropylene/6061 hybrid aluminium alloy FSP are as follows traverse speed was 40 mm / min, rotational speed was 1420rpm and tool tilt angle was 1 degree.
3. A significant volume of PP resin has flowed through aluminium alloying layer, needle-shape, honeycomb-style pores, forming several microstructures with corresponding enhanced binding properties, stir processing parameters with the application of maximum friction.
4. The most critical processing parameter was traverse speed, while the tool tilt angle had the least impact on tensile power.

5. Traverse speed, rotational speed, and tool tilt angle each contribute 78.68 percent, 13.67 percent, and 7.03 percent, respectively.
6. The findings have an important role to play in optimizing the polypropylene/6061 aluminium hybrid processing technique. Further work and improvements are required, however to apply outcomes to a specific type of polymer/metal.

### REFERENCES

- [1] Venkatesh, V.; Akhil, G.; Liang, G.; Rangarajan, V. Finite Element Based Physical Chemical Modeling of Corrosion in Magnesium Alloys. *Metals* 2017, 7, 83.
- [2] Ramani, K.; Tagle, J. Process-induced effects in thin-film bonding of PEKEKK in metal-polymer joints. *Polym. Compos.* 1996, 17, 879–885.
- [3] Grujicic, M.; Sellappan, V.; Omar, M.A.; Seyr, N.; Obieglo, A.; Erdmann, M.; Holzleitner, J. An overview of the polymer-to-metal direct-adhesion hybrid technologies for load-bearing automotive components. *J.Mater. Process. Tech.* 2008, 197, 363–373.
- [4] C. J. Dawes and W. M. Thomas, Friction stir process welds aluminium alloys, *Welding Journal*, 75 (3) (1996) 41-45.
- [5] G. Cam, Friction stir welded structural materials beyond Alalloys, *International Materials Reviews*, 56 (1) (2011) 1-48.
- [6] R. M. Leal, C. Leitao, A. Loureiro, D. M. Rodrigues and P. Vilaca, Material flow in heterogeneous FSW of thin aluminium sheets: Effect of shoulder geometry, *Journal of Materials Science and Engineering A*, 498 (2008) 384-391.
- [7] K. Kumar and S. V. Kailas, The role of friction stir welding tool on material flow and weld formation, *Journal of Materials Science and Engineering A*, 485 (2008) 367-374.
- [8] S. Rajakumar, C. Muralidharan and V. Balasubramanian, Predicting tensile strength, hardness and corrosion rate of friction stir welded AA6061-T6 aluminium alloy joints, *Materials and Design*, 32 (5) (2011) 2878-2890.
- [9] H. K. Rafi, G. D. J. Ram, G. Phanikumar and K. P. Rao, Microstructure and tensile properties of friction welded aluminium alloy AA7075-T6, *Materials and Design*, 31 (2010) 2375-2380.

- [10] V. Balasubramanian, Relationship between base metal properties and friction stir welding process parameters, *Journal of Materials Science and Engineering A*, 480 (2008) 397-403.
- [11] M. De Giorgi, A. Scialpi, F. W. Panella and L. A. C. De Filippis, Effect of shoulder geometry on residual stress and fatigue properties of AA6082 FSW joints, *Journal of Mechanical Science and Technology*, 23 (2009) 26-35.
- [12] A. R. Rose, K. Manisekar and V. Balasubramanian, Effect of axial force on microstructure and tensile properties of friction stir welded AZ61A magnesium alloy, *Transactions of Nonferrous Metals Society of China*, 21 (2011) 974-984.
- [13] A. J. Ramirez and M. C. Juhas, Microstructural evolution in Ti-6Al-4V friction stir welds, *Materials Science Forum*, 426-432 (2003) 2999-3004.
- [14] H. Fujii, L. Cui, N. Tsuji, M. Maeda, K. Nakata and K. Nogi, Friction stir welding of carbon steels, *Journal of Materials e and Engineering A*, 429 (2006) 50-57.
- [15] M. Amirizad, A. H. Kokabi, M. Abbasi Gharacheh, R. Sarrafi, B. Shalchi and M. Azizieh, Evaluation of microstructure and mechanical properties in friction stir welded A356+15%SiCp cast composite, *Materials Letters*, 60 (2006) 565-568.
- [16] A. Abdollah-Zadeh, T. Saeid and B. Sazgari, Microstructural and mechanical properties of friction stir welded aluminium/copper lap joints, *Journal of Alloys and Compounds*, 460 (2008) 535-538.
- [17] Y. C. Chen and K. Nakata, Friction stir lap joining aluminium and magnesium alloys, *Scripta Materialia*, 58 (2008) 433-436.
- [18] A. Arici and S. Mert, Friction stir spot welding of polypropylene, *Journal of Reinforced Plastics and Composites*, 27 (2008) 18.
- [19] M. K. Bilici, A. I. Yukler and M. Kurtulmus, The optimization of welding parameters for friction stir spot welding of high density polyethylene sheets, *Materials and Design*, 32 (2011) 4074-4079.
- [20] G. H. Payeganeh, N. B. Mostafa Arab, Y. Dadgar Asl, F. A. Ghasemi and M. Saeidi Boroujeni, Effects of friction stir welding process parameters on appearance and strength of polypropylene composite welds, *International Journal of the Physical Science*, 6 (19) (2011) 4595-4601.
- [21] S. K. Mazumdar and S. V. Hoa, Application of Taguchi method for process enhancement of on-line consolidation technique, *Composites*, 26 (1995) 669-763.
- [22] Li, X.; Gong, N.; Yang, C.; Zeng, S.; Fu, S.; Zhang, K. Aluminium/polypropylene composites produced through injection molding. *J. Mater. Process. Technol.* 2018, 225, 635–643.
- [23] Chen, J.; Du, K.; Chen, X.; Li, Y.; Huang, J.; Wu, Y.; Yang, C.; Xia, X. Influence of surface microstructure on bonding strength of modified Polypropylene/Aluminium alloy direct adhesion. *Appl. Surf. Sci.* 2019, 489, 392–402.
- [24] G. S. Peace, Taguchi methods, Addison-Wesley, New York, USA (1993).
- [25] Y. S. Tarn, S. C. Juang and C. H. Chang, The use of grey based Taguchi methods to determine submerged arc welding process parameters in hardfacing, *Journal of Materials Processing Technology*, 128 (2002) 1-6.
- [26] S. Neşeli, İ. Asiltürk and L. Çelik, Determining the optimum process parameter for grinding operations using robust process, *Journal of Mechanical Science and Technology*, 26 (11) (2012) 3587-3595.
- [27] M. W. Azizi, S. Belhadi, M. A. Yallese and T. M. JeanFrançois Rigal, Surface roughness and cutting forces modeling for optimization of machining condition in finish hard turning of AISI 52100 steel, *Journal of Mechanical Science and Technology*, 26 (12) (2012) 4105-4114.
- [28] H. S. Hong, T. Seo, D. Kim, S. Kim and J. Kim, Optimal design of hand-carrying rocker-bogie mechanism for stair climbing, *Journal of Mechanical Science and Technology*, 27 (1) (2013) 125-132.
- [29] N. Muhammad, Y. HP Manurung, M. Hafidzi, S. K. Abas, G. Tham and E. Haruman, Optimization and modeling of spot welding parameters with simultaneous multiple response consideration using multi-objective Taguchi method and RSM, *Journal of Mechanical Science and Technology*, 26 (8) (2012) 2365-2370.
- [30] S. C. Juang and Y. S. Tarn, Process parameter selection for optimizing the weld pool geometry in the tungsten inert gas welding of stainless steel,

- Journal of Materials Processing Technology, 122 (2002) 33-7.
- [31] H. Ahmadi, N. B. Mostafa Arab, F. Ashenai Ghasemi and R. Eslami Farsani, Influence of pin profile on quality of friction stir lap welds in carbon fiber reinforced polypropylene composite, *International Journal of Mechanics and Applications*, 2 (2012) 24-28.
- [32] G. Buffa, G. Campanile, L. Fratini and A. Prisco, Friction stir welding of lap joints: Influence of process parameters on the metallurgical and mechanical properties, *Journal of Materials Science and Engineering A*, 519 (2009) 19-26.
- [33] H. Ahmadi, N. B. M. Arab, F. A. Ghasemi and R. E. Farsani, Effect of pin geometry on surface appearance and tensile shear strength of friction stir polypropylene composite welds, *International Congress on AWST, Antalya, Turkey*, 24-25 October (2011).
- [34] R. B. Penteado, T. G. Hagui, J. C. Faria, M. B. Silva and M. V. Ribeiro, Application of Taguchi method in process improvement of turning of a Superalloy Nimonic 80A, *21st Annual Conference on Production and Operations Management Society POMS, Georgiam Hanna*, 1 (2010) 1-8.
- [35] ASTM Standard D5868, Standard test method for lap shear adhesion for fiber reinforced plastic (FRP), In: *Annual book of ASTM standard*, 15 (2002) 03.
- [36] P.J. Ross, *Taguchi techniques for quality engineering*, McGraw Hill, New York, USA (1988).
- [37] A. K. Lakshminarayana and V. Balasubramanian, Process parameters optimization for FSW of RDE-40 aluminium alloy using Taguchi technique, *Transactions of Nonferrous Metals Society of China*, 18 (2008) 548-554.
- [38] MINITABTM Statistical software Release 16.
- [39] A. G. Thakur, T. E. Rao, M. S. Mukhedkar and V. M. Nandedkar, Application of Taguchi method for resistance spot welding of galvanized steel, *Asian Research Publishing Network Journal of Engineering and Applied Sciences*, 5 (2010) 11.
- [40] Kimiaki, N.; Shoichiro, Y.; Atsuki, T. Direct joining of carbon-fiber-reinforced plastic to an aluminium alloy using friction lap joining. *Compos. Part B* 2015, 73, 82–88
- [41] Chen, M.A.; Li, H.Z.; Zhang, X.M. Improvement of shear strength of aluminium-polypropylene lap joints by grafting maleic anhydride onto polypropylene. *Int. J. Adhes. Adhes.* 2017, 27, 175–187.